Adsorption and regeneration of expanded graphite modified by CTAB-KBr/H₃PO₄ for marine oil pollution

Congbin Xu [a, b], Chunlei Jiao [a], Ruihua Yao [c], Aijun Lin [a, *], Wentao Jiao [d, **]

[a] College of Chemical Engineering, Beijing University of Chemical Technology, Beijing, 100029, China
[b] College of Resources and Environment, University of Chinese Academy of Sciences, Beijing 100049, China
[c] Chinese Academy for Environmental Planning, Beijing, 100012, China
[d] Research Center for Eco-Environmental Sciences, Chinese Academy of Sciences, Beijing, 100085, China

ARTICLE INFO

ABSTRACT

The cleaning-up of viscous oil spilled in ocean is a global challenge, especially in Bohai, due to its slow current movement and poor self-purification capacity. Frequent oil-spill accidents not only cause severe and long-term damages to marine ecosystems, but also lead to a great loss of valuable resources. To eliminate the environmental pollution of oil spills, an efficient and environment-friendly oil-recovery approach is necessary. In this study,[1]expanded graphite (EG) modified by CTAB-KBr/H₃PO₄ was synthesized via composite intercalation agents of CTAB-KBr and natural flake graphite, followed by the activation of phosphoric acid at low temperature. The resultant modified expanded graphite (M-EG) obtained an interconnected and continuous open microstructure with lower polarity surface, more and larger pores, and increased surface hydrophobicity. Due to these characteristics, M-EG exhibited a superior adsorption capacity towards marine oil. The saturated adsorption capacities of M-EG were as large as 7.44 g/g for engine oil, 6.12 g/g for crude oil, 5.34 g/g for diesel oil and 4.10 g/g for gasoline oil in 120min, exceeding the capacity of pristine EG. Furthermore, M-EG maintained good removal efficiency under different adsorption conditions, such as temperature, oil types, and sodium salt concentration. In addition, oils sorbed into M-EG could be recovered either by a simple compression or filtration-drying treatment with a recovery ratio of 58–83%. However, filtration-drying treatment shows better performance in preserving microstructures of M-EG, which ensures the adsorbents can be recycled several times. High removal capability, fast adsorption efficiency, excellent stability and good recycling performance make M-EG an ideal candidate for treating marine oil pollution in practical application.

1. Introduction

Marine oil pollution is one of the environmental concerns that are currently becoming major issues in the petroleum industry. Marine oil pollution may arise from oil run-offs from onshore facilities and from oil tanker spills during transportation (Drevon, 1992; Jackson et al., 1989; Jernelöv, 2010). Oil pollution has become severer with increasing petroleum activities. (Lan et al., 2015; Peterson et al., 2003). Between 2010 and 2015, spills from oil tankers alone contribute 33,000 tons of oil pollution in marine environment (Jin et al., 2017; Yuan et al., 2017). Consequently, the cleaning-up of viscous oil spills is a global challenge, especially in Bohai for the slow current movement and poor self-purification capacity.

Frequent oil-spill accidents not only cause severe and long-term damages to marine ecosystems, but also lead to a great loss of valuable resources (Jing et al., 2015; Lin, 2016). To eliminate the environmental pollution of oil spills quickly, an efficient and environment-friendly oil-recovery approach is highly demanded. Conventional methods for oil cleanup include sorption (Hubbe et al., 2013), manual skimming (Kinner et al., 2014), in situ burning (Prendergast and Gschwend, 2014), and bioremediation (Sarbatly et al., 2016). Among these treatment methods, adsorption has attracted much attention because of its high efficiency and ease to apply (Sun et al., 2013). Adsorbents sorbs contaminant molecules by providing large surface areas for physical or chemical interaction (Ding et al., 2015; Sun et al., 2014). Currently, the main limitations

for applying adsorbents in field remediation of contaminated sites are high capital cost and relatively low adsorption efficiency and capacity of sorbent materials.

Carbon-based materials are one of the most commonly used adsorbents. Among various carbon-based materials, activated carbon has already been widely used as sorbents in the treatment of oil pollution (Chang et al., 2007). Its relative low adsorption efficiency, however, limits its further applications. Although carbon nanotubes (Fard et al., 2016; Liu et al., 2014) and graphene (Wang et al., 2014) can provide high adsorption efficiency, they are too expensive to be used in applications such as oil cleanup. Expanded graphite (EG) is an inorganic porous carbon based adsorbent with a low density (0.002–0.010 g cm^{-3}), and is usually prepared from well-crystallized natural flake graphite (Chen et al., 2006). It is potentially an excellent inexpensive adsorbent with high porosity, weak polarity, hydrophobic nature and high oleophilic properties to different oils (Yao et al., 2016; Yue, 2011). In addition, EG causes no serious pollution to the environment, and can be easily disposed (Park et al., 2013). Despite the rising attention to EG, few people have applied it directly to the removal of marine oil because the preparation of EG is a high energy consumption process (Li et al., 2008) and its adsorption capacity is relatively low. Therefore, the modification of EG has become one of the important research fields for marine oil removing.

In the present research, expanded graphite was modified to reduce the preparation temperature and increase the ability to remove oils from ocean. To this aim, EG was modified by composite intercalation agent of CTAB-KBr, followed by the activation of phosphoric acid under low temperature, which has rarely been reported in the literature. The structural characteristics of EG before and after modification were evaluated via various techniques. In addition, a comprehensive set of experiments was performed in order to evaluate the adsorption and regeneration capability of EG modified by CTAB-KBr/H$_3$PO$_4$ (M-EG) for different oils of the Bohai Sea.

2. Experimental part

2.1. Materials

Natural flake graphite (99%, grain size 50 mesh) was purchased from Kim to Qingdao Graphite Co., Ltd, (China). Potassium permanganate (KMnO$_4$, ≥99.5%), nitric acid (HNO$_3$, 65%), phosphoric acid (H$_3$PO$_4$, 85%), acetic acid (CH$_3$COOH, 36%–38%) were supplied by Beijing Yili Fine Chemicals Co., Ltd (China). Cetyl trimethyl ammonium bromide (CTAB, ≥99.5%) and potassium bromide (KBr, ≥99.8%) was supplied by Beijing chemical Reagent Co., Ltd (China). The seawater used in the experiments was collected from the Bohai Sea, Tianjing, China.

2.2. Preparation of EG&M-EG

EG was synthesized by the following several steps. The mixed acid was prepared with perchloric acid and nitric acid at a ratio of 1:1.1.00 g of KMnO$_4$ was dissolved into the mixed acid, and then 10.00 g of natural flake graphite (NFG) was added to the solution. The graphite was oxidized for 5 h under continuous stirring. Afterwards, the resulting mixture was washed with water, the precipitate was filtered and dried at 70 °C for 40 min. The expandable graphite was prepared, and then expanded with muffle furnace at 900 °C to obtain EG.

The preparation process of M-EG was similar to that for EG (as described in Fig. 2). 2 ml of phosphoric acid was added to the mixed acid, and 6.00 g of CTAB and KBr was mixed in deionized water with a mass ratio of 1:1 to make CTAB-KBr composite modification

agent; then 10.00 g of expandable graphite was mixed with the compound modifier, stirred for 30 min and placed for 3 h, and then washed, dried and heated on a low-temperature furnace operated at 800 W for 20 s to obtain M-EG. The expanded volume was determined by measuring 1.0 g of the expanded graphite by graduated cylinder.

2.3. Characterizations

Both EG and M-EG samples were characterized by Scanning electron microscopy (SEM), specific surface area, FTIR spectra and XPS spectra. SEM (SU 8020) was operated at an acceleration voltage of 5 kV. Fourier transformed infrared (FT-IR) spectra of samples was recorded using a Thermo Nicolet NEXUS FI-IR spectrophotometer in the wave number range of 400–4000 cm^{-1} at a resolution of 4 cm^{-1} using the KBr pellet method. The XPS spectra of M-EG were obtained using an Amicus (Shimadzu Co., Japan) X-ray photoelectron spectroscopy. The specific surface areas of EG and M-EG were determined by N$_2$ Brunauer-Emmett-Teller adsorption analysis using a surface area analyzer (Nova, 2000e; Quantachrome Instrument, USA).

2.4. Batch adsorption experiment

The synthesized materials were tested for their capacity to remove oil from water using batch sorption experiments. Briefly, 100 ml of seawater was transferred to a 250 ml jar, and the sorbent materials were added to the seawater with various oil types, concentrations and temperatures. In order to simulate the real ocean situation, the mixture was placed on a shaker with a frequency of 70 cycles per minute. At the end of the experiment, the sorbent material was removed from the oil and water mixture, drained for 2 min in a filtration equipment, and weighed. The mass of water entrapped into the sorbent was determined by Karl Fischer titration following ASTM D1533.

For each experiment, the corresponding value of the adsorbed oil onto the adsorbent at equilibrium, Q$_e$, was calculated by subtracting the water content and the initial adsorbent weight from the total weight of the wet adsorbent:

$$Q_e = C_e - C_w - C_M \tag{1}$$

Where C$_e$ is the total weight (g) of oil, water and adsorbent material at equilibrium, measured gravimetrically. C$_w$ is the water weight (g) as determined by the Karl Fischer technique and C$_M$ is weight of the adsorbent material (g). In order to measure the amount of oil adsorbed onto the sorbent material at each specified of time, Q$_t$, Eq. (2) was given as follows:

$$Q_t = C_t - C_w - C_M \tag{2}$$

Where C$_t$ is the total weight (g) of oil, water and adsorbent material at time t.

3. Results and discussion

3.1. Characterization of EG and M-EG

In order to analyze EG before and after modification, corresponding characteristics were shown in Table 1. From the table, it can be seen that, despite the low working power M-EG required during preparation, M-EG obtained larger surface area and expanded volume than EG. In particular, the expanded volume achieved an increase of 100 mL/g. This increase can be explained by the change in pore structure before and after the modification by
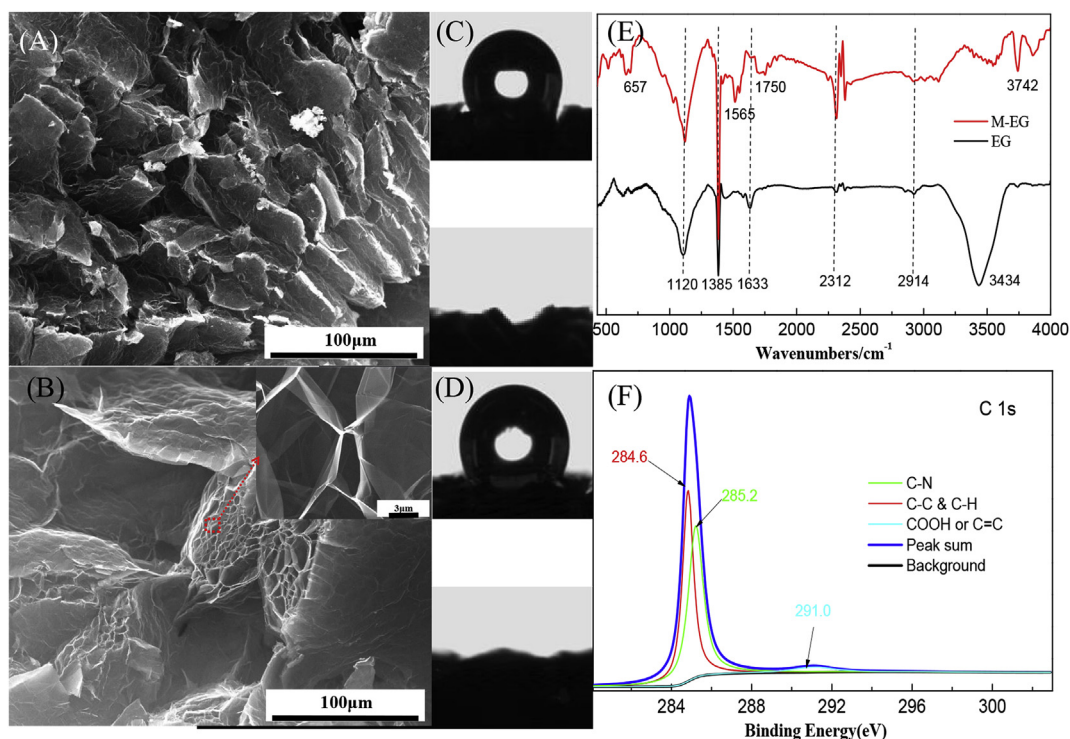
Fig. 1. Characterization of EG and M-EG (A)SEM image of EG; (B)SEM image of M-EG; (C) wettability measurement of EG; (D) wettability measurement of M-EG; (E) FT-IR spectra of EG and M-EG; (F) XPS spectra of M-EG.
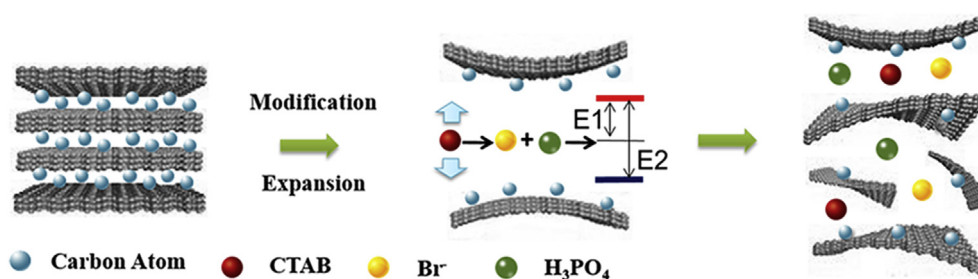
Fig. 2. Schematic illustration of modification mechanism.

Table 1
Characteristics of EG and M-EG

Preparation equipment	The resulting material	Working power(W)	Expanded volume (mL/g)	The specific surface area (m²/g)
Muffle furnace	EG	2000	290	219
Low-temperature furnace	M-EG	800	390	259

CTAB-KBr/H$_3$PO$_4$, suggested by the results from SEM. Consequently, M-EG, prepared by low temperature furnace, is energy saving and has better surface characteristics than EG.

The SEM micrographs of EG and M-EG in Fig. 1(A) and (B) show a more porous and uneven structure in samples post-modification. From the SEM image in Fig. 1(A), it can be seen that EG present a framework with the pore numbers ranging from hundreds to thousands, which are constructed by folds and open, semi-open type of pore structure on EG's surface. Such structure increases EG's surface and thus the pollutants can be adsorbed more easily under appropriate conditions. After treated with composite modification agents, as displayed in Fig. 1(B), M-EG still kept the uneven and porous structure. However, compared to the surface of EG, M-

EG architectures showed an interconnected and continuous open microstructure. The surface of M-EG has a honeycomb substructure with diamond-shaped pores, and graphite layers are mostly open. Compared to EG, slit-shaped holes were reduced or even disappeared, and polygonal pore structure was formed, which resulted in increased pore size and volume. The porous structure and plenty of the capillary interstices were revealed in the high magnification SEM image of Fig. 1(B), and the pore sizes vary from several microns to tens of microns. The result of pore structure analysis of M-EG indicates that the micropore volume and average pore size are up to 48.86 cm^3 g^{-1} and 87.84 nm, respectively. The special loosely bonded, porous and honeycomb structures that EG achieved post-modification provide it with high ability of sorption.

FTIR spectra of EG and M-EG are presented in Fig. 1(E) to elucidate the modification mechanism, a variety of functional groups of expanded graphite were detected by FTIR spectra. The broad band at 3434 cm^{-1} and the band at 1633 cm^{-1} found in EG could be attributed to the stretching vibrations of intra and inter-molecular hydrogen bonded −OH and C=C, respectively. The bands around 2914 cm^{-1} corresponded to the -CH$_2$ stretching vibrations, while the characteristic C−H peaks appeared at 1385 cm^{-1} for the -CH$_3$ group. The bands at 1120 cm^{-1} were attributed to the −CO stretching of the secondary alcohol, and the band at 2312 cm^{-1} indicated the presence of C=O bending. After modification, the characteristic peaks of EG at 3434 cm^{-1}, 2312 cm^{-1} and 1633 cm^{-1} almost disappeared. Meanwhile, new bands at 1570 cm^{-1} and 1720 cm^{-1} were ascribed to the stretching vibration of C=N and −COOH. In addition, the peaks of intermolecular hydrogen bonds at 3742 cm^{-1} and the peaks for C-Br at 657 cm^{-1} were also detected on M-EG. The FT-IR results indicated that compound modifier had been grafted on the surface of EG through intermolecular hydrogen bonded −OH groups, C=O groups and C=C bending.

To further investigate the chemical composition of the resulting M-EG, XPS measurements were performed, as shown in Fig. 1(F). The XPS analyses exhibited the XPS energy spectrum of C1s in M-EG. The characteristic peaks at 284.6 eV indicated the presence of C-C or C-H, and the band at 285.2 eV indicated C-N group. Furthermore, a weak peak for -COOH or C=C at 291.0 eV was also detected. Meanwhile, the band for C-O, C=O was not detected. In addition, elemental analysis showed that the amount of N and Br increased from 0.84% to 0−1.29% and 0.79%, respectively; while O decreased from 4.11% to 3.76% after the treatment by compound modifier. The XPS results indicated that chemical reactions occurred on the surface of EG, and oxygen functional groups were replaced by bromine or nitrogen functional groups. Importantly, the reduction of oxygen content on M-EG surface could lead to a decrease in polarity and an increase in hydrophobicity, which is good for oil-water separation.

The surface tension of EG and M-EG was tested by a water contact angle measurement. As shown in Fig. 1(C) and (D), The water contact angles of M-EG and EG were 135.6° and 129°, respectively, indicating that M-EG displayed stronger surface hydrophobicity than EG. Compared to hydrophobic wettability, both EG and M-EG showed excellent oleophilic property. After an engine oil droplet was dripped on the surface of EG and M-EG, it was absorbed immediately and a contact angle of oil of 0° was observed. Therefore, EG and M-EG displayed high hydrophobicity and super oleophilicity. However, M-EG showed stronger hydrophobicity than EG, which is consistent with the decreased polarity. Owing to above characteristics, M-EG exhibited excellent adsorption and oil-water separation performance.

Base on the above analysis, the speculation of modification mechanism is presented in Fig. 2. As a raw material for the synthesis of EG, nature flake graphite was compacted together. When synthesizing EG, due to the reaction between strong acid (HNO$_3$), oxidation agent (KMnO$_4$) and graphite layer, the distance between adjacent graphite was greatly increased, along with slight distortions. Consequently, expandable graphite was expanded at a high temperature, leading to the breakdown of the bonds between the interaction compounds and functional groups in EG.

Different from the synthesis of EG, M-EG underwent a further modification with CTAB-KBr and H$_3$PO$_4$, and this method of expansion costed less energy. Expandable graphite, the predecessor of EG, was prepared by NFG under the effect of oxidant and intercalation agent. The carbon element on the surface of NFG lost electrons to form positively charged carbon atom after oxidation (Liu and Yan, 2002). Due to the charge repulsion, the mutual exclusion between two positive charges of carbon opens the compact structure of NFC. In this study, we used the cationic surfactant of CTAB as the intercalation agent, different from the traditional anionic intercalation agent (Smith and Korgel, 2008). As one of the cationic surfactants, CTAB can further increase the charge repulsion between graphite layers.

However, two obstacles block the way to achieve the above process. First, CTAB and carbon atom have the same electronegativity, which makes it difficult for CTAB to be inserted into the graphite layers. Adding a certain amount of potassium bromide successfully solved the problem. Br$^-$ ionized by KBr could partially shield the positive charges of CTAB, which reduced the electrostatic repulsion of CTAB solution. With the effect of bromide ions, CTAB can penetrate deeper into graphite layers, making expansion effect more obvious and forming more active functional groups such as C=N and C-Br bond. Second, the activation energy of the above process is too high to achieve without catalytic agents. As a solution, the active agent phosphoric acid, was added and successfully lowered the activation energy, making it possible to prepare the composite modified expanded graphite by low-temperature furnace (Sirimuangjinda et al., 2012).

3.2. Removal performance of EG and M-EG towards marine oil

In order to be suitable for oil leakage accidents under seawater conditions, materials need to work effectively under high salinity system. In this regard, the adsorption of engine oil on M-EG under different sodium salt concentrations was investigated by batch experiments. As shown in Fig. 3(A), M-EG exhibited exceptional adsorption features for engine oil. The adsorption of engine oil on M-EG was observed to be independent from sodium salt concentration. The results indicated that M-EG was suitable for oil leakage accidents under high salinity conditions.

In order to highlight the superior performance of M-EG in removing different marine oils, we compared the adsorption capacity of EG before and after modification. The maximum adsorption capacity of EG and M-EG for engine oil, crude oil, diesel oil and gasoline oil is shown in Fig. 3(B). In our experiment, the maximum adsorption capacities of EG are 6.32, 5.54, 5.15 and 4.00 g/g and the maximum adsorption capacities of M-EG are 7.44, 6.12, 5.34 and 4.1 g/g respectively for engine oil, crude oil, diesel oil and gasoline oil. The results demonstrated that M-EG is a more efficient adsorbent to extract different oils from seawater. The excellent adsorption capacities for different oils of M-EG may be ascribed to the following synergistic effects. First, of the pore structure was changed in M-EG. With the effect of CTAB-KBr, expansion volume of EG increased with growth of pores inside the expanded graphite particles, which provided adequate transportation channels and facilitated the diffusion of oil from the exterior to interior sites on the adsorbent. Therefore, the larger expanded volume was, the higher sorption capacity of expanded graphite for marine oil obtained. Second, a large amount of CTAB cations available on the surface of M-EG provided more opportunities for the adsorption of negatively charged oil molecules through electrostatic attraction. Third, the correlation between the removal capacities and BET surface area, in which M-EG demonstrated enhanced removal capacities towards oil molecules over EG, indicates the extensive exposed outer surface is also thought to endow them with abundant adsorption sites available for oil molecules capture. On the other hand, M-EG has better hydrophobicity than EG, which is crucial for selective uptake of spilled oils. In addition, for M-EG, the adsorption capacity increased by 17.72%, 10.47%, 3.68% and 2.5% for engine oil, crude oil, diesel oil and gasoline oil, respectively. It could be explained by the different glutinosity and density properties of different oils. The viscosity and density of engine oil and crude oil are larger than that of diesel oil and gasoline.

The complexity of marine oil pollution in the practical operation
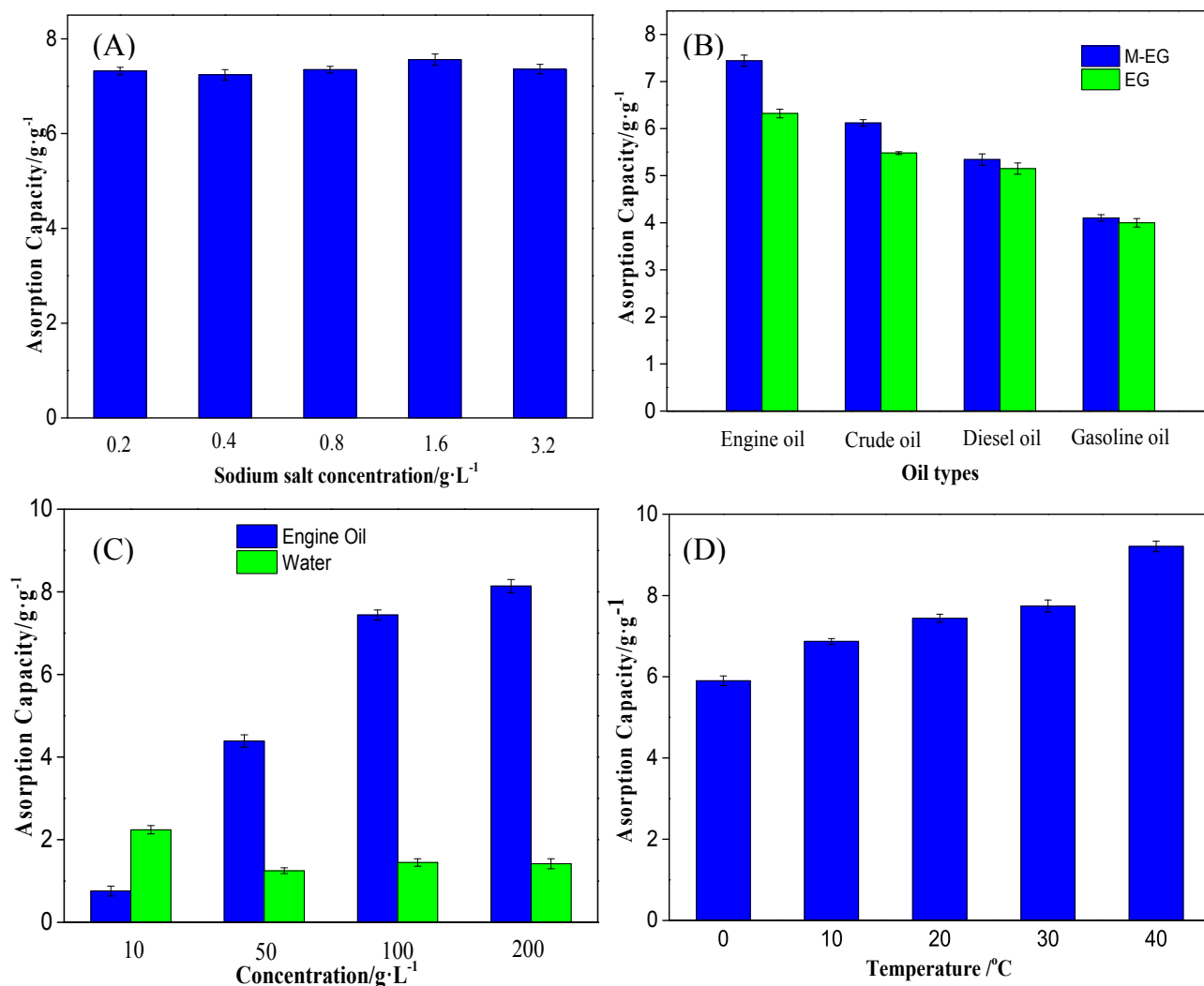
Fig. 3. (A) Sodium salt concentration effect on the removal of oil by M-EG; (B) Marine oil types effect on the removal performance by M-EG and EG; (C) Marine oil concentration effect on the removal performance by M-EG; (D) Temperature effect on the removal of marine oil by M-EG(initial concentration: 100 g/L; Temperature: 20 °C; Adsorbent dosage: 2 g/L; adsorption equilibrium time: 120min).

is beyond our imagination, since there are many external factors that interferes with the adsorption process. In this study, we examined the effect of engine oil concentration on the adsorption properties of M-EG. As shown in Fig. 3(C), increasing the concentration of engine oil can result in an increase in adsorption capacity of M-EG. This observation can be justified by the fact that both M-EG and oil are non-polar substances, which lead to great affinity to each other. Thus, M-EG has a preferential adsorption on oil, and the adsorption capacity of M-EG increases rapidly with the increase oil concentration. In addition, the amount of water adsorbed onto M-EG decreased sharply and then increased slightly. Since M-EG has a certain saturated adsorption capacity, the adsorption amount of water decreases with the increase of adsorption oil. However, when the amount of adsorbed oil increases to a certain extent, the amount of water adsorbed by M-EG may also increase slightly due to the presence of winding space, which is caused by EG deformation after oil absorption (Zheng et al., 2008). According to Zhou(Zhou et al., 2001), a model of winding space was built to analyze the oil absorption process of expanded graphite. They found that the oil adsorbed on the surface of EG was only about 40% of the total amount of oil adsorbed, and most of the rest went into the winding space or the hole inside. It is worth mentioning that

shaking by shaker enabled the molecules of oil to penetrate further into the adsorbent in this study when simulating the real marine environment, possibly because the surface area between oil molecules and M-EG was increased significantly by shaking.

The effect of temperature on the removal capacity of engine oil in seawater was investigated in the range of 0 °C–40 °C, which was used to imitate the real environment of the ocean. The results are shown in Fig. 3(D). Based on Fig. 3(D), the adsorption capacity of engine oil increased with rising temperature in the presence of M-EG. The adsorption capacity of M-EG was about 5.90 g/g at 0 °C, while the adsorption capacity of M-EG increased to 9.21 g/g at 40 °C. This can be explained that the adsorption of engine oil is an endothermic process, and the adsorption process of engine oil is promoted with the increase of temperature. In addition, this change in adsorption capacity may be related to the decrease in viscosity of engine oil with increasing temperature. When the temperature increases, the engine oil molecules diffuse to the surface of M-EG more rapidly, and the time required for reaching a state of equilibrium in the adsorption system is shorter at higher temperatures.

Overall, M-EG has high environmental performance, in which adsorption capacity of the material has changed within an
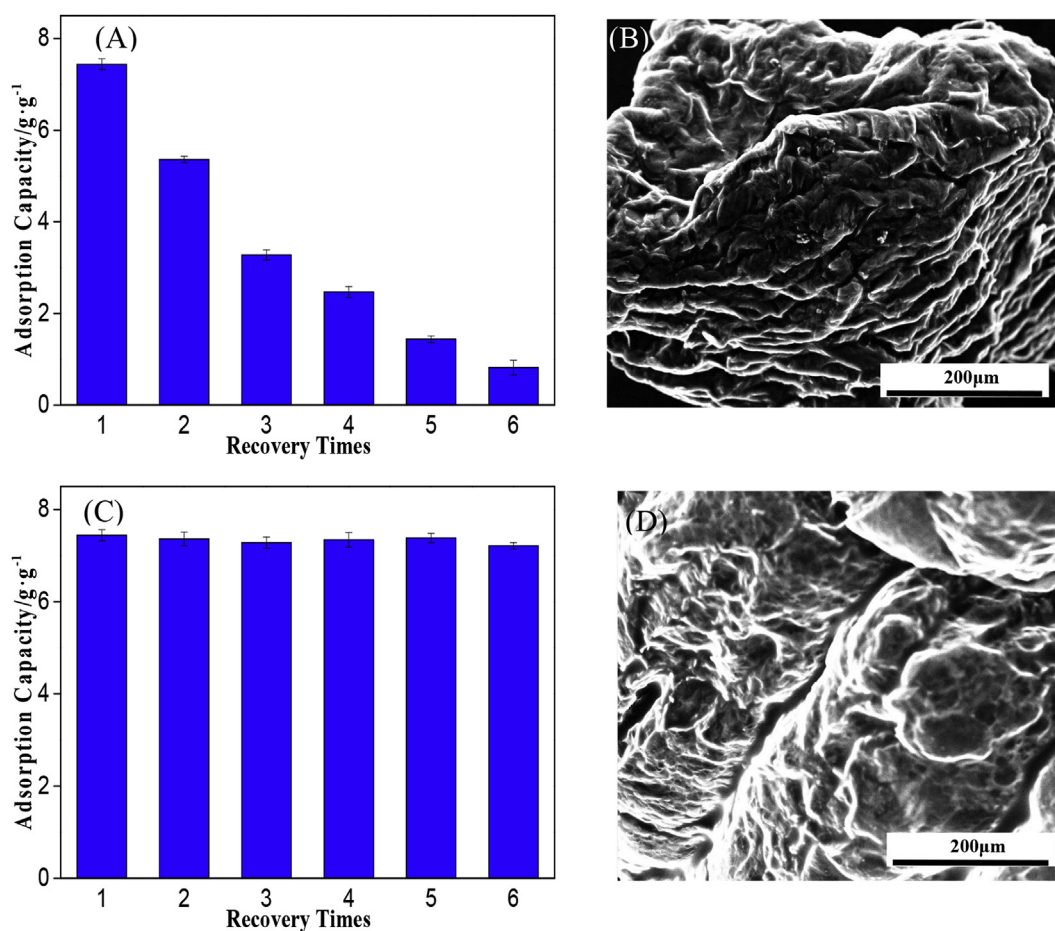
Fig. 4. (A) The adsorption recyclability of M-EG for marine oil with compression treatment over six cycles; (B) The adsorption recyclability of M-EG for marine oil with suction filtration treatment over six cycles; (C) SEM image of M-EG after cyclic utilization with compression treatment; (D) SEM image of M-EG after cyclic utilization with suction filtration treatment (initial concentration: 100 g/L; Temperature: 20 °C; Adsorbent dosage: 2 g/L; adsorption equilibrium time: 120min).

acceptable range in different environmental factors, and thereby further promotes the application of M-EG in marine oil pollution.

3.3. Recyclability and recoverability

High recyclability of the adsorbent and recoverability of oil are key requirements for practical oil cleanup applications. In this study, oil sorbed onto M-EG was recovered either by a simple compression or a filtration-drying cycle (Fig. 4). When M-EG was squeezed after sorbing engine oil to its maximum capacity, a large amount of engine oil came out from M-EG. However, it can be seen from Fig. 4(A) that the adsorption capacity of M-EG decreased significantly with the increase of cycle times. After compression, M-EG was broken into pieces and the characteristic texture of M-EG

was destroyed. And the bulk density became higher, and the porous structure of M-EG disappears (Fig. 4(B)). As a consequence, it's unfavorable to recycle M-EG by simple compression. Therefore, it was necessary to develop a much milder procedure for oil recovery in order to recycle M-EG.

Therefore, we adopted a simple filtration-drying cycle for recycling M-EG and recovering engine oil (Fig. 5). In this process, M-EG was first saturated with engine oil and then the majority of oil in the materials was separated by a suction filter under mild pressure. Finally, the materials were heated to the boiling point of engine oil. The vapor of engine oil was collected and condensed for recovery, while M-EG was regenerated. This process was repeated 6 times to determine recyclability (Fig. 4(C)). Over six repetitions, M-EG showed stable performance: M-EG adsorbed engine oil up to
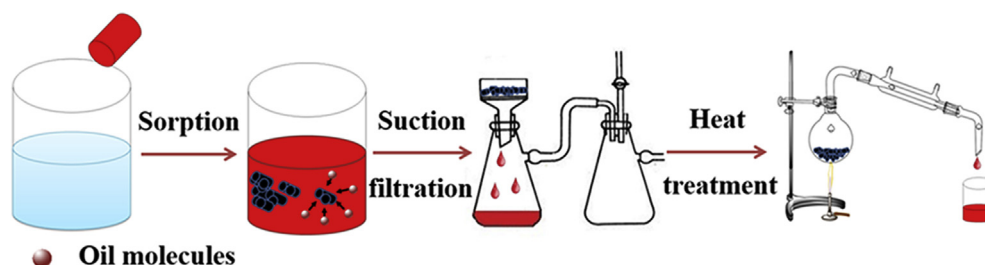
Fig. 5. Schematic diagram of the adsorption of marine oil and recyclability of expanded graphite by suction filtration and heat treatment.

over 6 times of its dry weight, and no obvious decrease of adsorption capacity was observed. The recovery yield of engine oil was close to 100% during this process. Therefore, by using a suction filtration and drying of the sorbed M-EG, engine oil was recovered without disrupting the microstructure of M-EG (Fig. 4(D)). Therefore, the honeycomb substructures with diamond-shaped pores were homogenously distributed on M-EG framework, which guaranteed the outstanding adsorption performance of M-EG towards oil from seawater after repeated use several times.

4. Conclusions

In summary, M-EG was successfully synthesized via the reaction between NFC, CTAB, KBr and H_3PO_4 with low-temperature furnace as the expanding equipment. The resultant M-EG has a homogeneously distributed honeycomb substructure with diamond-shaped pores. M-EG exhibited outstanding adsorption performances towards different oils in seawater due to the high surface-to-volume ratio and interconnected pore in the honeycomb substructure and the effect of CTAB-KBr. Besides high removal efficiency, M-EG demonstrated desirable environmental stability, good recycling performance, and easy separation operations. Therefore, M-EG could be an ideal candidate for treating marine oil pollution in practical application.

Acknowledgements

References

Chang, Y.U., Xian-Hui, L.I., Qiu, J.S., Sun, Y.F., 2007. Removal of sulfur-containing compounds from oil by activated carbon adsorption. J. Fuel Chem. Technol. 35, 121—124.

Chen, Z.G., Liu, C.B., Zhang, Y., Qiu, T., Liu, X., 2006. Dynamic adsorption of expanded graphite for oil in waste water of oil field. Mater. me. Eng. 30, 81—83.

Ding, C., Cheng, W., Sun, Y., Wang, X., 2015. Novel fungus-Fe$_3$O$_4$ bio-nanocomposites as high performance adsorbents for the removal of radionuclides. J. Hazard. Mater 295, 127—137.

Drevon, C.A., 1992. Marine oils and their effects. Nut. Rev. 50, 38—45.

Fard, A.K., Mckay, G., Manawi, Y., Malaibari, Z., Hussien, M.A., 2016. Outstanding adsorption performance of high aspect ratio and super-hydrophobic carbon nanotubes for oil removal. Chemosphere 164, 142—155.

Hubbe, M.A., Rojas, O.J., Fingas, M., Gupta, B.S., 2013. Cellulosic substrates for removal of pollutants from aqueous systems: a review. Bioresources 8, 3038—3097.

Jackson, J.B., Cubit, J.D., Keller, B.D., Batista, V., Burns, K., Caffey, H.M., Caldwell, R.L., Garrity, S.D., Getter, C.D., Gonzalez, C., 1989. Ecological effects of a major oil spill on panamanian coastal marine communities. Science 243, 37—44.

Jernelöv, A., 2010. How to defend against future oil spills. Nature 466, 182—183.

Jin, G., Luan, S., Wang, Y.C., Zhao, H.Y., Yao, H.B., Zhu, Y.B., Ye, Z., Zhu, H.W., Wu, H.A., Yu, S.H., 2017. Joule-heated graphene-wrapped sponge enables fast clean-up of viscous crude-oil spill. Nat. Nanotech.y 12, 434.

Jing, L.I., Gong, X., Qiao, D., Wang, B., Han, D.F., Zhang, X., 2015. Review of the impact of oil pollution on the food security of marine shellfish. Fis. Qual. Stand 01, 47—53.

Kinner, N.E., Belden, L., Kinner, P., 2014. Unexpected sink for deepwater horizon oil may influence future spill response. Eos. Trans. Am. Geo. Union 95, 176—176.

Lan, D., Liang, B., Bao, C., Ma, M., Xu, Y., Yu, C., 2015. Marine oil spill risk mapping for accidental pollution and its application in a coastal city. Mar. Pollut. Bull. 96, 220—225.

Li, M., Li, J.T., Sun, H.W., 2008. Sonochemical decolorization of acid black 210 in the presence of exfoliated graphite. Ultrason. Sonochem 15, 37—42.

Lin, M.C., 2016. Marine environmental protection: a highly efficient method of degradation of heavy oil pollution on coastal beaches. Hydrol. Curr. Res. 7, 231—233.

Liu, G.Q., Yan, M., 2002. The preparation of expanded graphitc using fine flaky graphite. New Carbon Mat. 17, 13—18.

Liu, T., Chen, S., Liu, H., 2014. Oil adsorption and reuse performance of multi-walled carbon nanotubes. Proc. Eng. 102, 1896—1902.

Park, S.J., Lee, S.Y., Kim, K.S., Jin, F.L., 2013. A novel drying process for oil adsorption of expanded graphite. Carbon Lett. 14, 193—195.

Peterson, C.H., Rice, S.D., Short, J.W., Esler, D., Bodkin, J.D., Ballachey, B.E., Irons, D.B., 2003. Long-term ecosystem response to Exxon Valdez oil spill. Science 302, 2082—2086.

Prendergast, D.P., Gschwend, P.M., 2014. Assessing the performance and cost of oil spill remediation technologies. J. Clean. Prod. 78, 233—242.

Sarbatly, R., Krishnaiah, D., Kamin, Z., 2016. A review of polymer nanofibres by electrospinning and their application in oil—water separation for cleaning up marine oil spills. Mar. Pollut. Bull. 106, 8.

Sirimuangjinda, A., Hemra, K., Atong, D., Pechyen, C., 2012. Production and characterization of activated carbon from waste tire by H3PO4 treatment for ethylene adsorbent used in active packaging. Adv. Mater. Res. 506, 214—217.

Smith, D.K., Korgel, B.A., 2008. The importance of the CTAB surfactant on the colloidal seed-mediated synthesis of gold nanorods. Langmuir. Acs J. Surf. Colloids 24, 644—649.

Sun, Y., Ding, C., Cheng, W., Wang, X., 2014. Simultaneous adsorption and reduction of U(VI) on reduced graphene oxide-supported nanoscale zerovalent iron. J. Hazard. Mater 280, 399—408.

Sun, Y., Shao, D., Chen, C., Yang, S., Wang, X., 2013. Highly efficient enrichment of radionuclides on graphene oxide-supported polyaniline. Environ. Sci. Technol. 47, 9904—9910.

Wang, N., Zhang, Y., Zhu, F., Li, J., Liu, S., Na, P., 2014. Adsorption of soluble oil from water to graphene. Environ. Sci. Pollut. Res. Int. 21, 6495.

Yao, T., Zhang, Y., Xiao, Y., Zhao, P., Guo, L., Yang, H., Li, F., 2016. The effect of environmental factors on the adsorption of lubricating oil onto expanded graphite. J. Mol. Liq. 218, 611—614.

Yuan, L., Han, L., Bo, W., Chen, H., Gao, W., Chen, B., 2017. Simulated oil release from oil-contaminated marine sediment in the Bohai Sea, China. Mar. Pollut. Bull. 118, 79—84.

Yue, X.Q., 2011. Effect of ZnO-loading method on adsorption and decomposition capacities of expanded graphite/ZnO composites for crude oil. Adv. Mater. Res. 284, 173—176.

Zheng, C.J., Xian-Ping, H.E., Yang, H.M., 2008. The unit root and cointegration tests for error correction models in panel data——based on the study on fiscal expenditure and economic growth in hubei province. J. Sci. Eng. 64, 87—92.

Zhou, W., Xiao fang, H.U., Dong, J., Zhao, H., Shen, W.C., Kang, F.Y., 2001. Behavior and mechanism of oil sorption on expanded graphitc. Technol. Water Treat. 16, 37—44.